Ultrafast Probing of Collective Electron Dynamics Driven by Dielectronic Repulsion

Ultrafast Probing of Collective Electron Dynamics Driven by Dielectronic Repulsion

M. A. Lysaght, P. G. Burke, and H. W. van der Hart

Centre for Theoretical Atomic, Molecular, and Optical Physics, Queen's University Belfast, Belfast BT7 1NN, United Kingdom

(Received 5 February 2009; published 15 May 2009)

We use the time-dependent R-matrix approach to investigate an ultrashort pump-probe scheme to observe collective electron dynamics in C^+. The ionization probability of a coherent superposition of the $2s2p^2\,{}^2D$ and ${}^2S$ states shows rapid modulation due to collective dynamics of the two equivalent $2p$ electrons, with the modulation frequency linked to the dielectronic repulsion. The best insight into this collective dynamics is achieved by a transformation from LS symmetry to the uncoupled basis. Such dynamics may be important in high-harmonic generation using open-shell atoms and ions.

DOI: 10.1103/PhysRevLett.102.193001 PACS numbers: 31.15.A−, 32.80.Qk, 32.80.Rm

The recent development of extreme ultraviolet (XUV) attosecond light pulses [1] has enabled research into ultrafast dynamics within atoms. Attosecond light pulses have, for example, been used in the real-time observation of shake-up processes in the double ionization of Ne [2], and in the formation of localized electron wave packets (EWPs) below the first ionization threshold of He [3], leading to the first observation of attosecond EWP interferences in a strongly driven atomic system. Electron dynamics deep inside an atom is also starting to attract significant interest, where, for example, theory has recently proposed a pump-probe scheme exploiting double ionization as a measure for the distance between electrons in superpositions of singly excited states of He [4].

One of the key questions regarding atomic physics on the ultrashort time scale is how the dielectronic repulsion between electrons affects the dynamics on the ultrashort time scale, and whether collective dynamics can actually be observed on this time scale. In this Letter, we propose an ultrafast pump-probe experiment in which collective dynamics between two equivalent electrons in an excited state of C^+ can be extracted. We demonstrate that a transformation from LS coupling to the uncoupled basis provides best insight, and will explain that collective dynamics can play a major role on the subfemtosecond time scale for general multielectron atoms.

In order to describe collective dynamics in a multielectron system, one needs to apply an approach capable of treating multielectron systems. The most sophisticated theoretical methods available to describe ultrafast electron dynamics are methods devoted to two-active-electron systems [4,5]. However, very few methods exist for treating general multielectron atoms irradiated by intense ultrashort light fields, and those that do typically employ the single-active-electron approximation [3]. Within the single-active-electron approximation, only the electron that is emitted is assumed to be active. As a consequence, ultrafast electron-electron interactions inside atoms have so far been investigated only to a limited extent. Most investigations have primarily focused on the influence of dielectronic interactions on two-photon double ionization of He [4,6–10]. In addition, electron-electron interactions have also been used to measure the distance between two electrons in He, by tracking the motion of a single excited electron [4]. In this study the motion under investigation can be explained within an single-active-electron framework.

The ultrafast pump-probe scheme for the current study of collective electron dynamics is similar to the scheme used in our previous study of ultrafast excitation dynamics in Ne [11]. This dynamics is induced by an XUV pump pulse, and the temporal evolution of this system is observed with a time-delayed ultrashort XUV probe pulse. The use of ultrashort pulses as a probe in such experiments offers the opportunity to monitor extremely fast dynamics in real time, and can in principle be used to capture dynamical electron correlation in atomic systems [4]. The basic features of the proposed experiment are explained schematically in Fig. 1. We consider a C^+ ion in its $2s^2 2p\,{}^2P^o$ ground state with total magnetic quantum number $M = 0$. This ion is excited by the first pulse, linearly polarized in the z direction, into a superposition

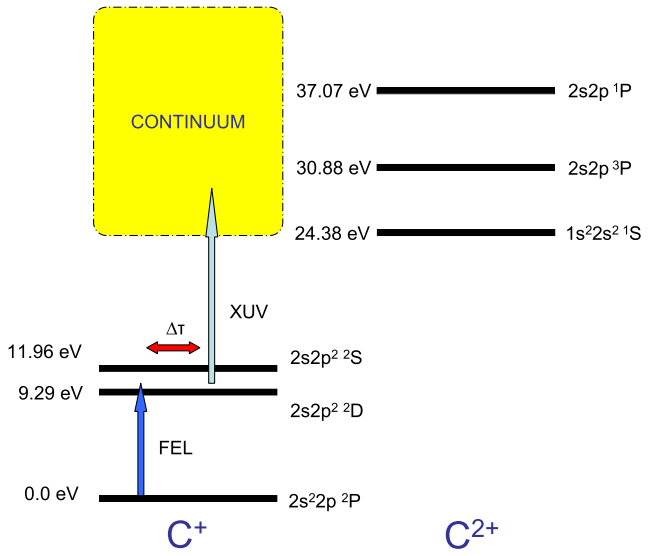

FIG. 1 (color online). Schematic of the proposed pump-probe experiment. FEL stands for free-electron laser.

of the $2s2p^2\,{}^2S^e$ and ${}^2D^e$ excited states. The energy separation between these two states, caused by the Coulomb repulsion between the two equivalent $2p$ electrons, results in a temporal interference between the two states with a frequency determined by the energy separation. In a naive single-configuration picture, the responsible dielectronic repulsion integral is the $F^2(2p, 2p)$ integral [12]. Hence, this repulsion governs the dynamical behavior of the EWP which continues to evolve after the end of the pump pulse. Subsequent irradiation of the C^+ ion with the time-delayed ultrashort pulse will ionize the C^+ ion. We study the ionization probability as a function of time delay between the two pulses to obtain information on the time-dependent interference between the ${}^2S$ and ${}^2D$ states and the associated electron dynamics.

The investigation is carried out using the recently developed three-dimensional time-dependent R-matrix theory [11]. This nonperturbative theory enables the interaction of ultrashort light fields with multielectron atoms and atomic ions to be determined from first principles, and was employed successfully to investigate ultrafast laser-driven excitation dynamics in Ne.

In the time-dependent R-matrix method, the solution of the time-dependent Schrödinger equation (TDSE) (in atomic units) at time $t = t_{q+1}$ is expressed in terms of the solution at $t = t_q$ as follows:

$$[H(t_{q+(1/2)}) - E]\Psi(\mathbf{X}_{N+1}, t_{q+1}) = \Theta(\mathbf{X}_{N+1}, t_q), \quad (1)$$

where

$$\Theta(\mathbf{X}_{N+1}, t_q) = -[H(t_{q+(1/2)}) + E]\Psi(\mathbf{X}_{N+1}, t_q). \quad (2)$$

In Eqs. (1) and (2) $\mathbf{X}_{N+1} \equiv \mathbf{x}_1, \mathbf{x}_2, \ldots, \mathbf{x}_{N+1}$ where $\mathbf{x}_i \equiv \mathbf{r}_i\sigma_i$ are the space and spin coordinates of the ith electron, and $H(t_{q+(1/2)})$ is the time-dependent Hamiltonian at the midpoint which is described in the length gauge throughout. In this formalism $E \equiv 2i\Delta t^{-1}$.

The solution of Eq. (1) is accomplished by partitioning configuration space into an internal and external region as in the standard R-matrix method [13] with the boundary at radius $r = a$. In the internal region electron exchange and electron-electron correlation effects between the ejected electron and the remaining N electrons are important, while in the external region such effects are negligible. Hence, the ejected electron moves in the local long-range potential of the residual N-electron atom or ion together with the laser field.

In the inner region $r \le a$, an R-matrix basis expansion of the wave function describing the $(N + 1)$-electron complex is adopted. The solution of a system of linear equations described in Ref. [11] at each time step enables the R matrix to be calculated on the boundary $r = a$ of this region and also enables the calculation of an inhomogeneous T vector which is due to the right-hand side of Eq. (1). In the outer region $a \le r \le a_p$, a set of coupled differential equations describing the motion of the scattered electron in the presence of the light field is solved at each time step by subdividing this region into n_s subregions and propagating the R matrix and T vector across them from $r = a$ to $r = a_p$. The R matrix and T vector at $r = a_p$ can then be used to propagate the wave function backwards across the n_s subregions. This propagated wave function then provides the starting point for the calculation at the next time step. A second R-matrix-based time-dependent approach has also been developed [14], but the dynamics within this approach is restricted to the R-matrix inner region only.

The structure of C^+ is described in the R-matrix internal region using the R-matrix basis developed for electron impact studies of C^{2+} [15], although we extend the inner region to a radius of 20 a.u., while the set of continuum orbitals contains 60 continuum functions for each available angular momentum of the continuum electron. The present calculations have been performed including the $1s^22s^2\,{}^1S^e$ ground state, and the $1s^22s2p\,{}^3P^o$ and ${}^1P^o$ excited states of C^{2+} as target states. The description of C^+ includes all $1s^22s^2\varepsilon l$ and $1s^22s2p\varepsilon l'$ channels up to $L_{\max} = 5$. In the external region we propagate the R matrix and T vector outwards to a radial distance of typically 1500 a.u. in order to prevent any reflections of the wave function from the external region boundary. Each external region sector is typically 3 a.u. wide and contains 35 B splines per channel with order $k = 9$.

The laser pulses used in the present investigation are as follows: The pump laser pulse has a central photon energy $\omega_1 = 10.88$ eV in order to be near resonant with the $2s2p^2\,{}^2S^e$ and ${}^2D^e$ states. It is defined by a three-cycle $\sin^2$ ramp on of the electric field followed by a three-cycle $\sin^2$ ramp off giving a pulse duration of 2 fs. The XUV ultrashort light pulse has a central photon energy $\omega_2 = 17$ eV and is also described by a three-cycle $\sin^2$ ramp on followed by a three-cycle $\sin^2$ ramp off of the electric field giving a pulse duration of 1.5 fs. Both pulses have a maximum intensity of 5×10^{12} W/cm^2.

Figure 2 shows the population in the $2s2p^2\,{}^2S$ and ${}^2D$ bound states as a function of time, where $t = 0$ is the start time of the pump pulse. It can be seen that the populations of $2s2p^2\,{}^2S$ and ${}^2D$ steadily increase during the pump pulse and evolve to a steady state after the end of the pump pulse. After letting the pumped C^+ freely evolve for $\sim$1 fs, we start to probe the bound state population from $\sim$3.8 fs onwards by irradiating C^+ at different delay times with an ultrashort XUV pulse that has a high enough photon energy (17 eV) to transfer the population in the excited states to the continuum. After the time-delayed ultrashort pulse, we allow the system to relax freely for $\sim$30 fs to enable the emitted electron to reach a distance of 200 a.u. This relaxation time also accounts for some decay of autoionizing states, but these could have lifetimes that are too long to fully take autoionization into account in a time-dependent calculation.

Figure 2 also shows the ionization probability due to the pulse sequence as a function of the time at which the probe

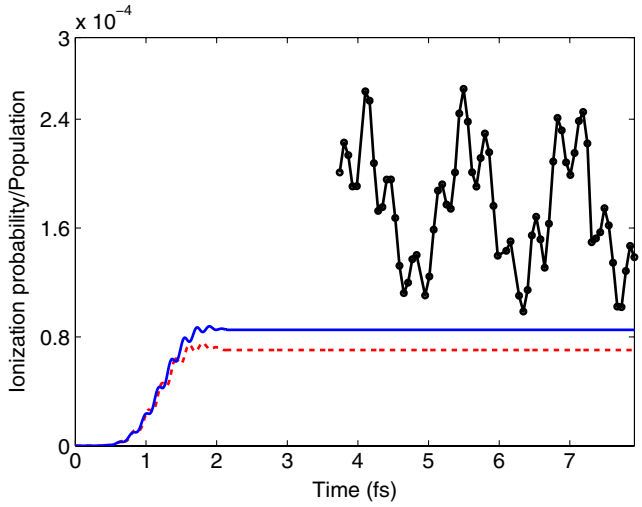

FIG. 2 (color online). Ionization probability (black joined dots) as a function of time, where time is measured at the moment at which the peak of the ultrashort probe pulse occurs with respect to the start time of the pump pulse. The $2s2p^2\,{}^2S$ population is shown as a dark gray (blue) solid line, and the $2s2p^2\,{}^2D$ population is shown as a light gray (red) dashed line. The bound state populations are shown here without the presence of the ultrashort pulse to show how the system freely evolves in time. The populations are scaled by a factor of 2×10^{-2}.

pulse reaches its peak intensity with respect to the start time of the pump pulse. The ionization probability is calculated by integrating the wave function in a spatial region given by 200 a.u. $< r <$ 1500 a.u.. We find that the ionization probability oscillates with a period, $T_{\mathrm{osc}} =$ 1.5 fs. These ultrafast oscillations can be accounted for by the fact that the probe pulse is probing an EWP in a superposition of the $2s2p^2\,{}^2S$ and ${}^2D$ excited states. These states are separated by an energy of $\Delta E \sim 2.4$ eV due to the electron-electron interaction between the two $2p$ electrons, and it is this interaction that leads to the interference between the two excited states. The oscillations with a period of ~0.4 fs are due to interferences between the two excited states and the ground state and are not of interest in this study.

Although the interference can be explained by the energy separation between the two states, this separation does not explain the ultrafast atomic dynamics in detail. The EWP generated here is primarily confined to the $2s2p^2$ configurations. Its dynamics is thus governed by angular dynamics, for which the main driver is the difference in electron-electron repulsion between the $2p$ electrons for $2s2p^2\,{}^2S$ and ${}^2D$. The LS coupled basis in which the atomic structure is described is, however, not the ideal basis to gain insight into this angular dynamics. To elucidate the dynamics, we thus transform from the LS coupled basis to the uncoupled basis $|2p_{m_1} 2p_{m_2}\rangle$, in which the role of magnetic substates becomes more transparent. Since we consider light polarized in the z direction, the total magnetic number M is conserved, $M = 0$. The $2s$ electron can be considered as a spectator electron, so that the LS coupled $2p^2\,{}^1S$ and ${}^1D$ configurations can be decomposed as follows:

$$|2p_0, 2p_0\rangle = -\sqrt{\tfrac{1}{3}}|2p^2\,{}^1S\rangle + \sqrt{\tfrac{2}{3}}2p^2|{}^1D\rangle, \quad (3a)$$

$$|2p_1, 2p_{-1}\rangle_S = \sqrt{\tfrac{2}{3}}|2p^2\,{}^1S\rangle + \sqrt{\tfrac{1}{3}}|2p^2\,{}^1D\rangle, \quad (3b)$$

where the subscript S indicates singlet spin coupling between the $m = 1$ and $m = -1$ electrons. This decomposition immediately suggests that angular dynamics in the $2s2p^2$ configuration involves collective dynamics of the two electrons: if the m value of one electron changes, the other electron must also experience a change.

We can now transform the description of the atomic structure from the LS coupling scheme to an uncoupled basis. This transformation only applies to the contribution of the $2s2p^2$ configuration to the state labeled $2s2p^2$. Other configurations also play a role, but they are far less important. Figure 3 again shows the ionization probability as a function of time delay, but this time the probability is compared to the population of the uncoupled basis functions. The first feature to note in Fig. 3 is that the population of $|2p_0, 2p_0\rangle$ shows small rapid oscillations for $t < 1.6$ fs, whereas the population of $|2p_1, 2p_{-1}\rangle_S$ does not. This is as expected. The C^+ $1s^2 2s^2 2p$ $M = 0$ ground state is dominated by electrons with $m = 0$. With the polarization of the laser pulse in the z direction, leading to $\Delta m = 0$, one should expect the interaction with $|2p_0, 2p_0\rangle$ to be stronger than with $|2p_1, 2p_{-1}\rangle_S$. The most striking feature in Fig. 3, however, is the periodic oscillation in the population of $|2p_0, 2p_0\rangle$ and $|2p_1, 2p_{-1}\rangle_S$. These oscillations closely match the observed oscillation in the ionization probability, with the oscillations of $|2p_0, 2p_0\rangle$ in phase. Hence the uncoupled basis provides a clearer interpretation of the ultrafast dynamics of C^+ explored here.

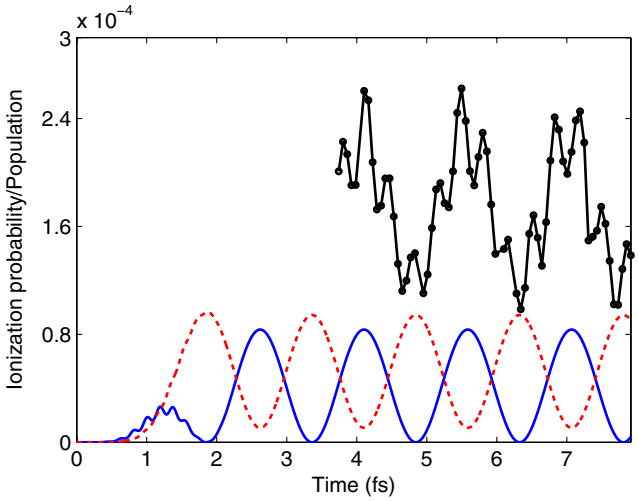

FIG. 3 (color online). Ionization probability (black joined dots) as a function of time, as shown in Fig. 2. Both the $|2p_0, 2p_0\rangle$ population (blue solid line) and the summed $|2p_1, 2p_{-1}\rangle_S$ population (red dashed line) are shown. The bound state populations are scaled as in Fig. 2.

The transformation into the uncoupled basis allows an assessment of the reasons why the ionization probability oscillates with time delay between the pump and the probe pulse. After the C^+ system has been excited by the pump pulse, the excited multielectron wave packet is in a breathing motion between two different angular distributions. When the population of $|2p_0, 2p_0\rangle$ has reached its maximum, the EWP is aligned along the direction of laser polarization, and so the probe pulse interacts strongly with the EWP, corresponding to a maximum in the ionization probability. Alternatively, when the population of $|2p_1, 2p_{-1}\rangle_S$ has reached a maximum, the EWP is aligned perpendicular to the direction of laser polarization, and so the probe pulse interacts less strongly with the EWP, resulting in ionization being suppressed. This scheme thus allows the observation of collective breathing motions in superpositions of low-lying atomic states, while the frequency of these motions is a measure of the magnitude of dielectronic repulsion.

This collective dynamics within the $2p^2$ states is of wider relevance to intense-laser physics. The dominant ionization mechanism for infrared laser fields is the sequential emission of $m = 0$ electrons. In this picture, emission of two electrons from Ne would lead to a Ne^{2+} ion with two $m = 0$ vacancies in the $2p$ shell. This hole then evolves like the $2p^2$ states of C^+ in this study. Hence, in Ne^{2+}, the $m = 0$ vacancies would be filled by an $m = 1$ and an $m = -1$ electron, and vice versa, which will effectively enhance ionization of the Ne^{2+} ion. If ionization is slow compared to the period of this transfer (1.1 fs for Ne^{2+}), the appropriate ionization rate to use for ionization of Ne^+ to Ne^{5+} is the ionization rate assuming the presence of a single $m = 0$ electron in the $2p$ shell. The dominance of the emission of electrons with $m = 0$ has already been demonstrated [16,17], but the results presented here may indicate the mechanism by which the $m = 0$ levels are filled and depleted. However, it must be noted that not all spin symmetries of the Ne ions are accessible by sequential emission of $m = 0$ electrons [18].

These observations also have implications for high-harmonic generation (HHG) from open-shell ions such as Ne^+ and Ar^+ [19]. High-harmonic generation is typically described by a three-step model, in which the laser field first ionizes the atom and accelerates the liberated electron away from and back into the core, generating high-harmonic photons when the returning electron recombines with the parent ion. Typically, high harmonics are generated from neutral noble-gas atoms, but they could in principle also be generated from open-shell systems. Suppose that we have Ne^+ in $M = 0$. In the first step an $m = 0$ electron is liberated, leaving the Ne^{2+} core in a superposition of $2s^2 2p^4\ ^1D$ and ^1S. This superposition will initially be in a $|2p_0, 2p_0\rangle$ hole, due to the absence of two $m = 0$ electrons (and hence ^3P is spin forbidden). Because of the energy gap between ^1D and ^1S, this superposition will now transform into a $|2p_1, 2p_{-1}\rangle_S$ hole and back. If the motion of the liberated electron is independent from the core, it will continue to have $m = 0$. If this electron returns when the core is in a $|2p_0, 2p_0\rangle$ hole, recombination is possible, but when the core is in a $|2p_1, 2p_{-1}\rangle_S$ hole, recombination is impossible as there is no $m = 0$ vacancy. Hence the present results suggest that angular core dynamics may have an influence on high-harmonic generation yields in open-shell systems.

In conclusion, we have demonstrated that ultrafast pump-probe techniques can be exploited to observe rapid oscillations in the ionization probability of C^+ due to collective electron dynamics. The uncoupled-electron basis provides a clearer interpretation of the ionization probability than the traditional LS-coupling scheme. The rapid oscillations in the ionization probability are ascribed to a breathing motion between two different angular distributions, explaining the modulation of the ionization yield as a function of time delay between the pump and probe pulse. The frequency of this oscillation is, in a naive picture, directly related to a particular electron-electron repulsion integral, $F^2(2p, 2p)$. This breathing motion between angular distributions could be a general feature of the multielectron response to strong laser fields, and could have a significant effect on multiple ionization and on the generation of high-harmonic radiation from open-shell systems. Direct experimental verification of the current theoretical results will, however, require high-density pure ion sources which is still a challenging problem.

M. A. L. acknowledges support through the UK EPSRC.

[1] M. Hentschel *et al.*, Nature (London) **414**, 509 (2001).
[2] M. Uiberacker *et al.*, Nature (London) **446**, 627 (2007).
[3] P. Johnsson *et al.*, Phys. Rev. Lett. **99**, 233001 (2007).
[4] S. X. Hu and L. A. Collins, Phys. Rev. Lett. **96**, 073004 (2006).
[5] J. S. Parker *et al.*, Phys. Rev. Lett. **96**, 133001 (2006).
[6] S. X. Hu, J. Colgan, and L. A. Collins, J. Phys. B **38**, L35 (2005).
[7] R. Shakeshaft, Phys. Rev. A **76**, 063405 (2007).
[8] I. A. Ivanov and A. S. Kheifets, Phys. Rev. A **75**, 033411 (2007).
[9] I. F. Barna, J. Wang, and J. Burgdörfer, Phys. Rev. A **73**, 023402 (2006).
[10] E. Foumouo *et al.*, New J. Phys. **10**, 025 017 (2008).
[11] M. A. Lysaght, P. G. Burke, and H. W. van der Hart, Phys. Rev. Lett. **101**, 253001 (2008).
[12] C. F. Fischer, T. Brage, and P. Jönsson, *Computational Atomic Structure: An MCHF Approach* (IOP, Bristol, 1997), Chap. 2.2.2.
[13] P. G. Burke and K. A. Berrington, *Atomic and Molecular Processes: An R-Matrix Approach* (IOP, Bristol, 1993).
[14] X. Guan *et al.*, Phys. Rev. A **78**, 053402 (2008).
[15] K. A. Berrington *et al.*, J. Phys. B **22**, 665 (1989).
[16] E. Gubbini *et al.*, Phys. Rev. Lett. **94**, 053602 (2005).
[17] R. Taïeb, V. Véniard, and M. Maquet, Phys. Rev. Lett. **87**, 053002 (2001).
[18] H. W. van der Hart, Phys. Rev. A **74**, 053406 (2006).
[19] E. A. Gibson *et al.*, Phys. Rev. Lett. **92**, 033001 (2004).